Performance Measurement of a Two-Stage Two-Bladed Savonius Rotor

K.K. Sharma*, R. Gupta*, A.Biswas*‡

*Mechanical Engg. NIT Silchar, Assam, India

(kksharma1313@rediffmail.com, r_guptanitsil@yahoo.com, agniab@rediffmail.com)

‡ Corresponding Author; K.K. Sharma, Mechanical Engg. NIT Silchar, Assam, India, kksharma1313@rediffmail.com

Received: 16.12.2013 Accepted: 11.01.2014

Abstract- Conventional Savonius rotor is the ancient form of Vertical Axis Wind Turbines (VAWT) rotor which has many advantages such as self-starting, omni-directional, less noisy, suitability for applications like pumping, grinding, sailing etc. However, its efficiency is only in the range of 15%-21%. Investigations are being conducted to improve its efficiency by controlling its design parameters. In this paper the performance of a two-stage two-bladed configuration of the Savonius rotor has been investigated. Experiments are conducted in a subsonic wind tunnel available in the department. The parameters studied are overlap, tip speed ratio, power coefficient (C_p) and torque coefficient (C_t). Overlap ratio of the design was optimized to generate maximum performance of the rotor. The study showed that a maximum C_p of 0.517 was obtained at 9.37% overlap condition. Thus C_p of the rotor is much higher than the conventional Savonius rotor.

Keywords- Two-stage Savonius rotor, overlap, tip speed ratio, power coefficient, torque coefficient

1. Introduction

Savonius rotor, also called S-rotor, was originally invented and patented by Finnish Engineer Sigurd J. Savonius in 1931. The concept of Savonius rotor is based on the principle of Flettner rotor, which is formed by cutting a cylinder into two halves along the central plane and then moving the two semi- cylindrical surfaces sideways along the cutting plane to resemble the letter `S`. Savonius [1] investigated the performances of 30 different models of the S-rotors in the wind tunnel. He reported a maximum power coefficient (C_p) of 0.31. Following Savonius, Bach [2] made some investigations of the Savonius rotor and related machines. The highest measured efficiency was 24%. Between Sixties and the last decade, many researchers [3-16] had investigated experimentally the performances of different designs of Savonius rotor and obtained their C_p in the range of 0.15-0.38. The efficiency of wind rotor depends on the overlap ratio between the buckets as well. Savonius [1] reported that maximum power coefficient at an overlap ratio of 0.25 is about three times that at zero overlap ratio. Bach G. [2] obtained maximum power coefficient in the overlap range of 0.20-0.25. Biswas et al. [16] obtained maximum power coefficient at the overlap of 0.20. Recently, some works had been done on the design improvements of the conventional Savonius rotor. Research work of Grinspan et al. [9] led to the development of a new blade shape with twist for the Savonius rotor. They obtained a maximum power coefficient of 0.5. Following Grinspan, Saha & Rajkumar [10] researched on twist bladed metallic S-rotor and compared the performance with conventional semicircular blades having no twist. However, the highest efficiency was reported to be only 0.14. Kamoji et al. [17] evaluated the performance of helical design of Savonius rotor in an open jet wind tunnel and compared the performance with that of conventional Savonius rotor. Atlan and Atilgan [18] in their research on design improvement of Savonius rotor proposed a curtain design that shields the return blade thereby creating a converging section in front of the rotor and increasing the wind speed entering the rotor. Power coefficients obtained (C_p= 0.4) was higher than the curtain-less design. Thus, there has been resurgence in the interest of Vertical Axis Wind Turbine (VAWT) rotors particularly the Savonius type rotor, which has increasingly been utilized for power production in small scale manner for domestic purpose in the built environment. Abraham et al. [19] investigated the potential of different designs of Savonius rotors for satisfying local energy demands. They also analyzed different methods to optimize Savonius rotor for providing power to mobile communication tower in

developing countries. Plourde et al. [20] investigated venting and capping on a novel VAWT rotor for powering mobile communication towers. Again Plourde et al. [21] designed a novel VAWT rotor for powering electrical units of mobile communication towers. Roy and Saha [22] analyzed the effects of some influencing parameters like curtain design, deflector plate, nozzle, ducts, shielding etc. as measures for improving the performance of Savonius rotor which would make them viable for small-scale applications in low wind conditions, and reported C_p could be as high as 0.38 due to these enhancements. Altan and Atilgan [23] investigated the performance of static torque of a conventional Savonius rotor by placing a curtain in front of the rotor and reported low static torque with short curtain dimensions and high static torque with long curtain dimensions. Again Rajkumar and Saha [24] performed low speed wind tunnel testing for evaluating the performance of a twist bladed Savonius rotor with non-return valves inside the concave side of the blades and reported improvement in the specific rotor output.

From the above discussions it is seen that performance of Savonius rotor can be increased by incorporating ad hoc tricks in the form of end plates, deflector plates, curtains, shielding, guide vanes etc in their designs, but these make the system structurally complex. However, multi-staging of conventional VAWT rotors [25] could be a viable proposition in terms of improvement of power output and hence efficiency. In this paper, an experimental investigation on the performance of a two-stage two-bladed Savonius rotor has been made with respect to overlap variation in the range between 9.37 % and 19.87%. Experiments were performed in an open circuit subsonic wind tunnel.

2. Physical Model

The model of two-stage two-bladed Savonius rotor is designed and fabricated in the workshop of the department. In each stage, the blades of the Savonius rotor are 8 cm in chord, 3 mm in thickness and 10 cm in height. Therefore, height of the full rotor is 20 cm. The top stage of the Savonius rotor is mounted 90^0 out of phase with respect to the bottom stage of the rotor. The rotor is mounted on a central shaft of 1.5 cm diameter and 25 cm height, supported by ball bearings in a circular base as shown in fig.1. The base is 9.2 cm in diameter and 2.8 cm thick. Washers & nuts having knurled surfaces are used to create overlap in the blades of the Savonius. Overlap is the distance of the inner edge of the blade from the axis of rotation assuming the arc is carried to the full semi-circle. Four overlap conditions namely 9.37%, 12.37%, 16.87% and 19.87% are obtained.

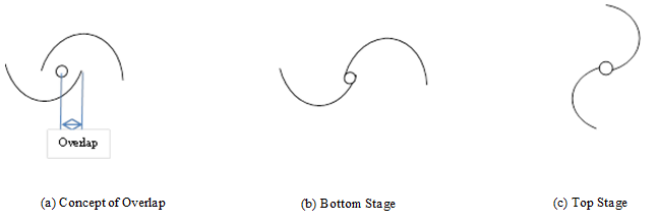

(a) Concept of Overlap (b) Bottom Stage (c) Top Stage

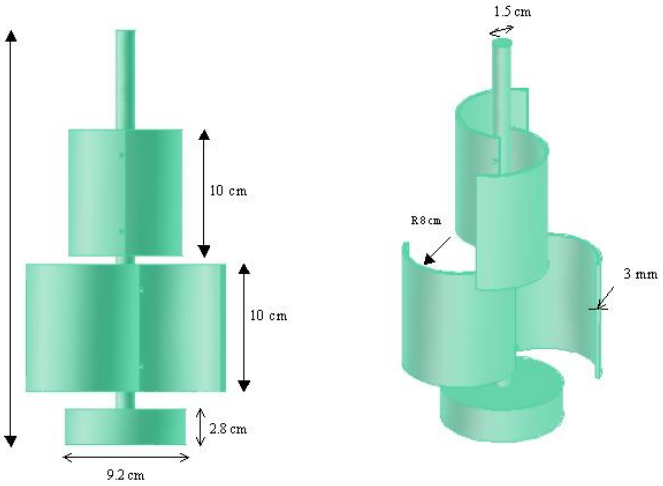

(d) Two stages assembled with dimensions

Fig. 1. Physical model of 2-stage 2-bladed Savonius rotor

3. The Wind Tunnel

Experiments were conducted in an open circuit subsonic wind tunnel (fig.2a). The size of the wind tunnel test section is 30 cm x 30 cm, and length of the test section was 3 metres. The operating range of the wind tunnel is zero to 35 m/sec. The wind tunnel had a centrifugal blower having 15 kW capacity motor with axial flow fan that supplied 6700 cubic feet per meter at rated 2890 rpm. The turbulence intensity of the wind tunnel is around $\pm$ 1%.The brief description of the subsonic wind tunnel can be found in the literature [26].

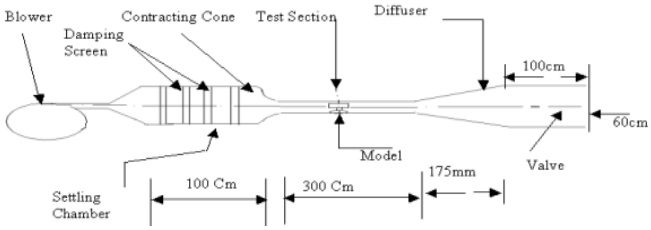

Fig. 2a. Schematic layout of open circuit subsonic wind tunnel

4. Experimental Description

From the experiments conducted in the wind tunnel, power coefficients of the rotor at different tip speed ratios for each overlap condition are determined. Power coefficient (C_p) is the ratio of power produced by the rotor to the maximum wind power for the same swept area (Eqn.1). The power produced by the rotor, P_{rotor}, is calculated as the product of aerodynamic force transmitted by the bucket of the rotor ($1/2\ \rho A V_1^2$) and blade speed, u, as given in Eqn.2. The aerodynamic force is measured as the ratio of rate of change of angular momentum of wind at inlet of the test section, i.e. the driving torque, to the radius of the rotor. It is understandable that wake is formed on the downstream of the rotor. Its velocity in the expression of Eqn 2 is neglected since it refers to the velocity deficit on the immediate downstream of the rotor as useful power extraction by a rotor lowers the velocity in the near wake. Hence it is taken as

zero. Practically also, the velocity in that zone is found to be less than unity; hence square of the same is more close to zero. Moreover readings are repeated number of times to ensure repeatability of the obtained values. In the calculation of rotor power, P_{rotor}, wind speed at inlet to rotor, V_1, is recorded by a pitot-static tube connected to a U-tube manometer while the blade speed is recorded using a digital tachometer of least count 1 rpm. The location in the test section where V_1 is recorded can be seen from fig.2b. The aerodynamic torque (T) is calculated from the standard relationship of power and torque (Eqn.6). Torque coefficient is calculated as the ratio of power coefficient to the tip speed ratio (Eqn.7). Tip speed ratio is calculated as the ratio of bladed speed to free stream wind speed (Eqn.8).

The performance of a wind rotor can be expressed in the form of power coefficient (C_p) versus Tip Speed Ratio, TSR (λ), and the torque coefficient (C_t) versus TSR at various overlap ratio conditions. For analysis, the following relations have been used.

$$C_p = \frac{P_{rotor}}{P_{\max}} \tag{1}$$

$$P_{rotor} = \left(\frac{1}{2}\rho A V_1^2\right) u = \left(\frac{1}{2}\rho A V_1^2\right)\frac{\pi DN}{60} \tag{2}$$

$$P_{\max} = \frac{1}{2}\rho A V_{free\_block}^3 \tag{3}$$

Where V_{free_block} is the free stream wind speed with blockage as given by the following relation:

$$V_{free\_block} = V_{free} * (1+\varepsilon) \tag{4}$$

Where 'ε' is the wind tunnel blockage correction factor due to combined solid and wake blockages. In the present rotor, the blockage ratio is 32.2%, and the corresponding blockage correction factor, ε, applied is 40% (27). When a rotor is placed in the test section of wind tunnel, it creates blockage to the flow, which increases the local free stream wind speed in the test section. In eqn 4, V_{free} is the free stream wind speed, which is recorded without placing the rotor inside the test section. The free stream wind speed with blockage, V_{free_block}, is recorded by placing the rotor inside the test section. The location in the test section where V_{free} and V_{free_block} are recorded can be seen from fig.2b. As seen from fig.2b, the location of free stream wind speeds is at much upstream than the location of wind speed at inlet to the turbine (V_1). This is so taken such that the free stream flow parameters are not distorted by the interactions of blades and wind at the rotor. It is further seen from fig.2(b) that wind speed at inlet to the test section, V_1, is recorded at a distance 4 cm from the blade tips so as to nullify the effect of blade tip losses. In wind tunnel testing, the blockage effect (Eqn.5) needs to be taken into account to determine the actual power produced by the rotor (28). The total blockage correction factor due to combined solid and wake blockages is given as

$$\varepsilon = \frac{1}{4}\frac{HD}{H'W} \tag{5}$$

$$T = \frac{60 P_{rotor}}{2\pi N} \tag{6}$$

$$C_t = \frac{C_p}{\lambda} \tag{7}$$

$$\lambda = \frac{u}{V_{free}} \tag{8}$$

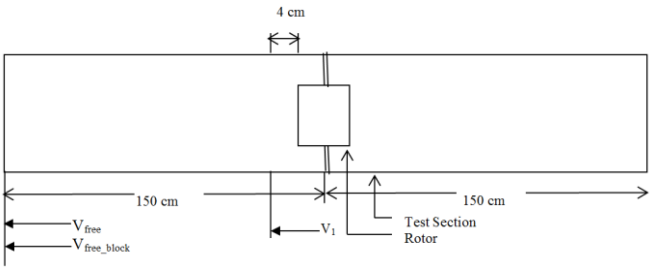

Fig. 2(b). Locations of various wind speed recordings in the wind tunnel test section

5. Experimental Results

The experimental results of the rotor are obtained for four overlap conditions namely 9.37%, 12.37%, 16.87% and 19.87%**.** The variations of power and torque coefficients with Tip Speed Ratio (TSR) at different overlap conditions are shown in fig.3 to fig.6.

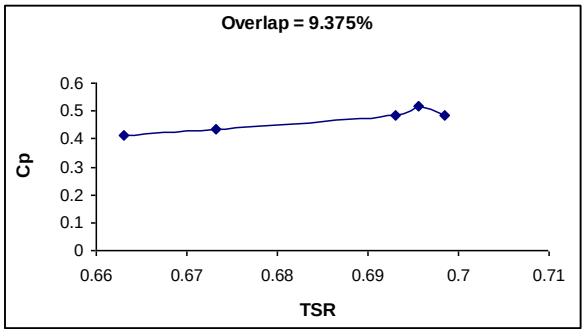

Fig. 3(a). Variation of C_p with TSR for 2-stage 2-bladed Savonius rotor at 9.37% overlap

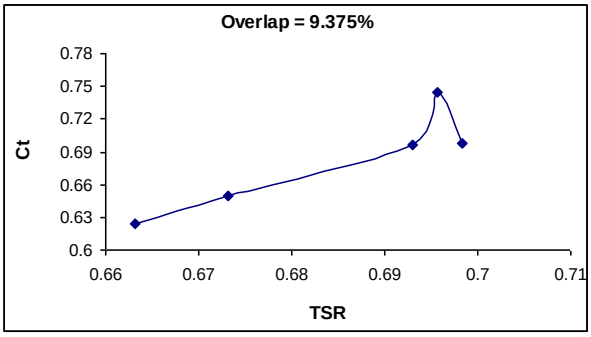

Fig. 3(b). Variation of C_t with TSR for 2-stage 2-bladed Savonius rotor at 9.37% overlap

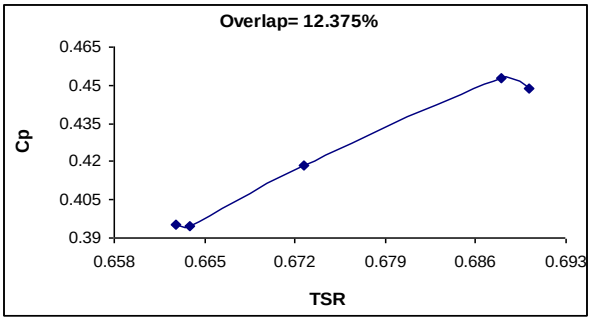

Fig. 4(a). Variation of C_p with TSR for 2-Stage 2-bladed Savonius rotor at 12.37% overlap

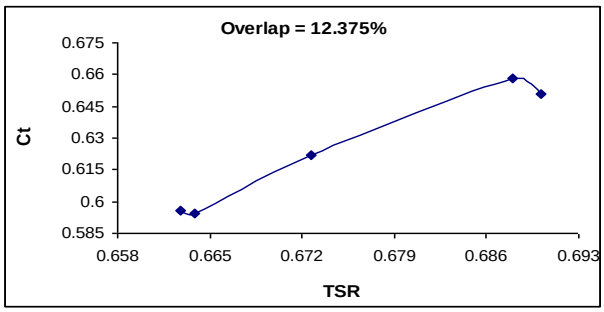

Fig. 4(b). Variation of C_t with TSR for 2-Stage 2-bladed Savonius rotor at 12.37% overlap

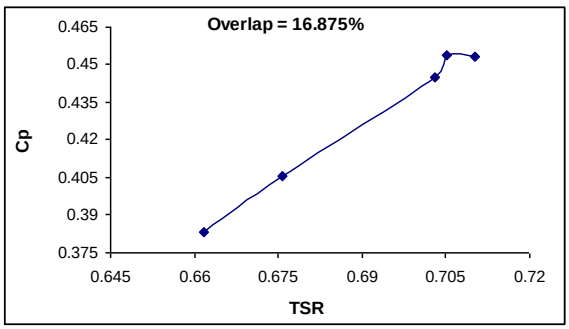

Fig. 5(a). Variation of C_p with TSR for 2-stage 2-bladed Savonius rotor at 16.87% overlap

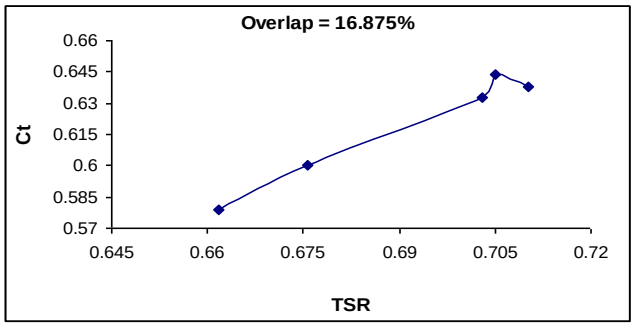

Fig. 5(b). Variation of C_t with TSR for 2-stage 2-bladed Savonius rotor at 16.87% overlap

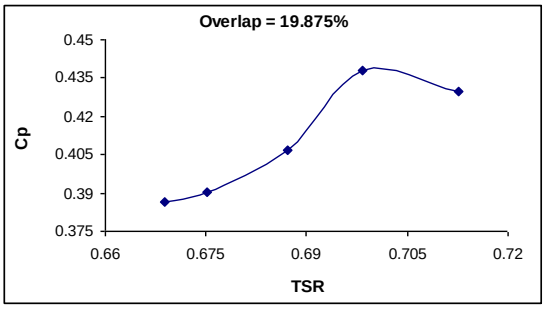

Fig. 6(a). Variation of C_p with TSR for 2-Stage 2-bladed Savonius rotor at 19.87% overlap

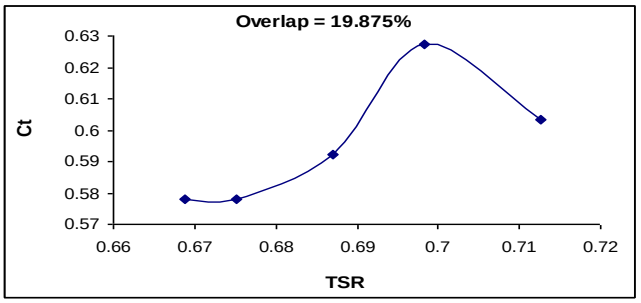

Fig. 6(b). Variation of C_t with TSR for 2-Stage 2-bladed Savonius rotor at 19.87% overlap

The plots showing the variations of performance coefficients with respect to Tip Speed Ratio (TSR) show that both power and torque coefficients increase with the increase of Tip Speed Ratio (TSR) up to certain limit and then decrease with further increase of the latter. Thus it can be concluded that there are optimum values of TSR for which the power & torque coefficient are the maximum. For 9.37% overlap, the maximum C_p of 0.514 is obtained at a TSR of 0.695 (fig.3a), and the maximum C_t of 0.744 is obtained at a same TSR of 0.695 (fig.3b). For 12.37% overlap, the maximum C_p of 0.453 is obtained at a TSR of 0.688 (fig.4a), and the maximum C_t of 0.658 is obtained at a same TSR of 0.688 (fig.4b). For 16.87% overlap, the maximum C_p of 0.45 is obtained at a TSR of 0.70 (fig.5a), and the maximum C_t of 0.64 is obtained at a same TSR of 0.70 (fig.5b). For 19.87% overlap, the maximum C_p of 0.438 is obtained at a TSR of 0.698 (fig.6a), and the maximum C_t of 0.627 is obtained at a same TSR of 0.698 (fig.6b). Therefore, power coefficient (C_p) decreases with the increase of overlap ratio from 9.37% to 19.87%. Thus there is an optimum value of overlap ratio for which the power coefficient is the maximum. The highest C_p of 0.517 is obtained at 9.37% overlap and at 0.695 TSR. The highest C_t of 0.744 is obtained at the same overlap of 9.37% and at 0.695 TSR. Further, the highest C_p and C_t are obtained at the same TSR for any overlap condition. And the optimum TSR at which these coefficients are obtained is close to a same value of 0.7.

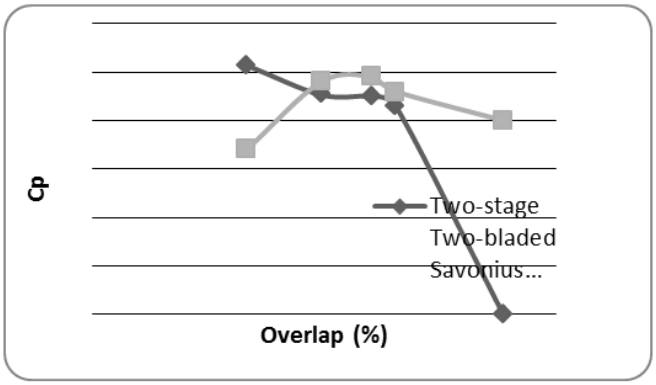

Fig. 7(a). Comparison of C_p with respect to overlap between single stage Savonius rotor and two-stage Savonius rotor

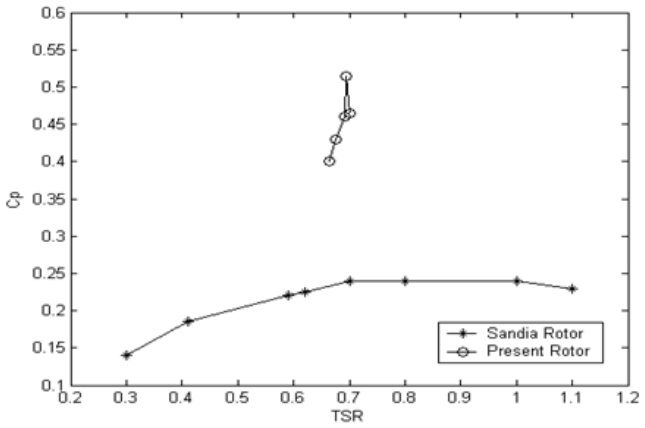

Fig. 7(b). Comparison of C_p with respect to TSR between Sandia Laboratories result & present result

Figure 7(a) shows the comparison of power coefficient with respect to percentage overlap between the present two-stage two-bladed Savonius rotor and a single stage two-bladed Savonius rotor having the same aspect ratio and both tested under identical experimental conditions [29]. The rotor aspect ratios are same since their heights are also same (i.e. 20 cm) and rotor diameters being same as the overlap values are same. However, with the present two-stage design, the stage aspect ratio drops as the height of each stage is now only 10 cm.

Now it can be seen from Fig. 7(a) that C_p of the present rotor for all overlap values other than 9.37% are lower than those of single stage two-bladed Savonius rotor. The reason is the lower value of aspect ratio for the present rotor, also explained in literature [30]. Therefore, the results obtained in the present paper for the two-stage rotor follows the same physics as discussed in the above literature. As far as the knowledge of the authors, in none of the literatures till date the performance of two or multi stage Savonius rotor designs was investigated for overlap condition in the stages as low as 9.37%. Perhaps the guidelines of optimum overlap condition [2,7], i.e. 15% to 25%, for single stage Savonius rotor could be partly responsible for that. However, C_p being higher for 9.37% overlap could be explained from the aerodynamic behaviour of the individual rotor stages. The top stage of the Savonius rotor is mounted 90^0 out of phase with respect to the bottom stage. Thus full projected cross-sectional area of the advancing blade is swept by the upstream wind compared to the bottom stage as wind strikes normal to the advancing blade, thereby extracting more energy from wind by virtue of the disposition of the top stage. And low overlap condition in the rotor stabilizes the Coanda flow [31] through the overlap, thus causing high power coefficient of the rotor at that overlap condition. But as the overlap increases beyond that, these aerodynamic advantages would be circumvented by the effect of circulation across the overlap [31], hence becoming responsible for the drop in C_p. Similar physics was also reported in a wind tunnel investigation of a combined Savonius and Darrieus rotor [25] with Savonius mounted on top, where C_p was reported to be highest at 0.51 for low overlap condition; but C_p dropped as the overlap got increased. As the advancing blade of the top stage reaches downstream, the bottom stage, being 90^0 out of phase, presents the concave face of its advancing blade at normal incidence before the wind thereby maintaining the cycle. However more investigations on the flow visualization study may be required for the present rotor to arrive at more concrete conclusions about its high C_p value at low overlap conditions.

Now to validate the results of C_p for the present rotor and to get an idea about the TSR values at which the C_p peaks occur, the variation of C_p with respect to TSR at the optimum overlap for the present two-stage two-bladed Savonius rotor is compared with that of single stage two-bladed Savonius rotor, as plotted in Fig.7(b). For comparison, the experimental results of C_p are taken from the work of Sandia Laboratories [32] in which a two-bladed Savonius rotor of aspect ratio unity and overlap variation 10% was considered. The present values of C_p correspond to those for 9.37% overlap condition. The Reynolds number for the present rotor is around 1.87×10^5, and for the Sandia rotor it was 4.37×10^5. In the present case, the highest C_p (0.514) is obtained at about 0.695 TSR, and their highest C_p (0.24) peaks at around 0.8 TSR as seen from Fig.7 (b). The range of TSR and the value of TSR at peak C_p for the Sandia laboratories' rotor are greater than the present rotor due to the effect of lower Reynolds number in the present case.

6. Conclusion

From the present investigation, the following conclusions can be summarized:

i) Both power and torque coefficients increase with the increase of TSR up to the maximum and then both decrease with further increase of the latter. Therefore there is an optimum TSR at which the performance coefficients are the highest.

ii) Similarly power and torque coefficients decrease with the increase of overlap from 9.37% to 19.87%.

iii) The maximum C_p of 0.514 is obtained at a TSR of 0.695 at an optimum 9.37% overlap, which is much higher than the conventional Savonius rotor.

iv) The highest C_t of 0.744 is obtained at the same overlap of 9.37% and at 0.695 TSR. Further, the highest C_p and C_t are obtained at the same TSR for any overlap condition. And the optimum TSR at which these coefficients are obtained is close to a same value of 0.7.

v) Lower value of C_p at high overlap condition is attributed to the low value of stage aspect ratio. Highest value of C_p at low overlap condition of 9.37% can be attributed to the combined effect of the disposition of the stages and also to the stabilization of Coanda flow across such small overlap, thereby negating the effect of low stage aspect ratio at this overlap.

Future work could entail investigation of the effect of different overlap conditions for individual rotor stages, within the given range of overlap conditions, on the performance of the present rotor. Effect of flow pulsations is to be studied to learn more on the aerodynamics of such rotor under unsteady condition. Actual wind rotor test is to be conducted in open air by scaling up the rotor to know its practical performances. Once performance is confirmed, for real world situation, a geometrically similar prototype of the rotor at the optimum overlap value can be fabricated and installed for use in varied applications like pumping, grinding, sailing etc.

References

[1] Savonius, S.J.: The S-turbine and its applications. Mech. Engg., 53(5), 333–338 (1931)

[2] Bach,G.,"Investigation Concerning Savonius rotors and related Machines". Translate into English by Brace Research Institute.,Quebec,Canada,1931.

[3] Mcpherson,R.B.(1972)."Design, Development and testing of Low Head High Power coefficient Kinetic Energy Machine". M.Sc Thesis, University of Massachusetts, Amherst, M.A.

[4] Newman, B.G. (1974). "Measurement on a Savonius rotor with variable gap". Proceeding Sherbrook University Symposium on wind energy', Sherbrook Canada, p-116.

[5] Khan, M.H. (1975)."Improvement of Savonius Rotor-windmill". M.S. thesis, University of the Phillipines, Lasbonas.

[6] Modi, V.J.; Roth, N.J.; Fernando, M.S.U.K., "Optimal configuration studies and prototype design of a wind energy operated irrigation system". Journal of Wind Engg & Industrial Aerodynamics, Vol.16, 1984, p 85-96.

[7] Sivasegaram, S., "Secondary parameters affecting the performance of resistance type vertical axis wind rotors". Journal of Wind Engg, Vol. 2, 1978, p 49-58.

[8] Khan, M.H., "Model & prototype performance characteristics of S-rotor wind mills". Journal of Wind Engg. Vol. 12, 1988, p 59-75.

[9] Grinspan, A.S.; Kumar, P.S.; Mahanta, P.; Saha, U.K.; Rao, D.V.R.; Bhanu, G.V. (2001). "Design, development & testing of Savonius wind turbine rotor with twisted blades". Proceedings 28th National Conference on Fluid Mechanics and Fluid Power, Dec 13-15, Chandigarh, p 428-431.

[10] Saha, U.K.; Rajkumar, M.J., "On the performance analysis of Savonius rotor with twisted blades". Journal of Renewable Energy, Vol.31, No.11, 2006, p 1776-1788.

[11] Modi, V.J.; Fernando, M.S.U.K., "On the performance of the Savonius wind turbine". ASME Journal of Solar Engg. Vol. 11, 1989, p 71-76.

[12] Alexander, A.J.; Holownia, B.P., "Wind tunnel tests on a Savonius turbine". Journal of Industrial Aerodynamics, Vol. 3, 1978, p 343-351.

[13] Saylers, A.T., "Blade configuration optimization & performance characteristics of a simple Savonius rotor". Journal of Institute of Mechanical Engineers, Vol. 199, 1985, p 185-191.

[14] Blackwell, B.F.; Sheldahl, R.E.; Feltz, L.V., "Wind tunnel performance data for two & three bucket S-rotors". Journal of Energy, Vol. 2, 1978, p 160-164.

[15] Sharma K.K., Gupta R., Singh S. K. and Singh S. R., Experimental investigation of the characteristics of a Savonius wind turbine, Wind Engineering, Vol 29 issue 1, 2005, pp 77-82.

[16] Biswas A., Gupta R., Sharma KK., Experimental Investigation of Overlap and Blockage Effects on Three-Bucket Savonius Rotors, Wind Engineering, vol. 31, no. 5, 2007 pp 363–368.

[17] Kamoji MA, Kedare SB, Prabhu SV. Performance tests on helical Savonius rotors. Renewable Energy, vol 34, no. 3, 2008, pp 521–9.

[18] Atlan B.D., Atilgan M., The use of a curtain design to increase the performance level of a Savonius wind rotors, Renewable Energy, vol 35, 2010, pp 821-829.

[19] J. P. Abraham, B.D. Plourde, G.S. Mowry, W.J. Minkowycz, Summary of Savonius Wind Turbine Development and Future Applications for Small-Scale Power Generation, Journal of Renewable and Sustainable Energy, Vol. 4, paper no. 042703, 2012.

[20] B. D. Plourde, J. P. Abraham, G. S. Mowry, and W. J. Minkowycz, An Experimental Investigation of a Large, Vertical-Axis Wind Turbine: Effects of Venting and Capping, Wind Engineering, Vol. 35, pp. 213-220, 2011.

[21] B. D. Plourde, J. P. Abraham, G.S. Mowry, W.J. Minkowycz, Use of Small-Scale Wind Energy to Power Cellular Communication Equipment, Sensors and Transducers, Vol. 13, pp. 53-61, 2011.

[22] S. Roy and U. Saha, Review of experimental investigations into the design, performance and optimization of the Savonius rotor, J. Power and Energy, 2013.

[23] B. Altan and M. Atilgan, An Experimental and Numerical Study on the Improvement of the Performance of Savonius Wind Rotor, Journal of Energy Conversion and Management, 49, 3425-2432 (2008).

[24] M.J. Rajkumar and U.K. Saha, Valve-Aided Twisted Savonius Rotor, Wind Engineering, 30, 243-254 (2006).

[25] Gupta, R., Biswas, A., Sharma, K.K.: Comparative study of three-bucket Savonius turbine with combined three-bucket-Savonius-three-bladed-Darrieus turbine, Journal of Renewable Energy, 33, 1974–1981 (2008).

[26] Gupta R., Das, R., Sharma, K.K.: Experimental study of a Savonius-Darrieus wind machine. In: Proceedings of the International Conference on Renewable Energy for Developing Countries, University of Columbia, Washington DC, 2006.

[27] A.J. Alexander and B.P. Holownia. Wind tunnel tests on a Savonius rotor. Journal of Industrial Aerodynamics, 3 (1978) 343—351.

[28] J. Abraham, G. Mowry, B. Plourde, Numerical Simulation of Fluid Flow Around a Vertical-Axis Wind Turbine, J. Renewable and Sustainable Energy, Vol. 3, p.033109, 2011.

[29] Sharma K.K (2012). Performance analysis of Savonius rotor and combination of Savonius Darrieus rotors through experimental and computational approaches. Dissertation, PhD, NIT Silchar, Silchar (India).

[30] M. A. Kamoji, M.A., Kedare S.B., Prabhu, S.V. Experimental investigations on single stage, two stage and three stage conventional Savonius rotor. International Journal of Energy Research, Volume 32, Issue 10, pages 877–895, 2008.

[31] Fujisawa, F. On the torque mechanism of Savonius rotor. Journal of wind Engg. & Industrial Aerodynamics, 40, 277- 292, (1992).

[32] Ben F. Blackwell, Robert E. Sheldahl, Louis V. Feltz. Wind Tunnel Performance Data for TWO- and Three-Bucket Savonius Rotors. Sandia Laboratories' Report, Report No. SAND 76-0131, July 1977.